Integrated turning-ray and reflection tomography for velocity model building in foothill areas

Tian Jun[1], Peng Gengxin[1], Junru Jiao[2], Grace (Yan) Yan[2], and Xianhuai Zhu[2]

Abstract

A special challenge for land seismic exploration is estimating velocities, in part due to complex near-surface structures, and in some instances because of rugose topography over foothills. We have developed an integrated turning-ray and reflection-tomographic method to face this challenge. First, turning-ray tomography is performed to derive a near-surface velocity-depth model. Then, we combine the near-surface model with the initial-subsurface model. Taking the combined model as starting model, we go through a reflection tomographic process to build the model for imaging. During reflection tomography, the near-surface model and subsurface models are jointly updated. Our method has been successfully applied to a 2D complex synthetic data example and a 3D field data example. The results demonstrate that our method derives a very decent model even when there is no reflection information available in a few hundred meters underneath the surface. Joint tomography can lead to geologic plausible models and produce subsurface images with high fidelity.

Introduction

Reflection tomography in the postmigration domain has dominated the advantages of velocity model building in seismic imaging, especially for marine seismic exploration in which the near-surface model is not problematic. Reflection tomography is challenged to derive a near-surface model with high quality because there are only very limited valid traces, or no valid traces, in the near surface up to a few hundred meters deep from the surface. An alternative method is desirable to obtain a reliable near-surface velocity-depth model. Here, we propose the integrated method of turning-ray tomography and reflection tomography to build velocity model for foothill exploration. First, we pick first breaks as the input for turning-ray tomography to derive the near-surface velocity-depth model. An initial subsurface depth model is obtained by converting root mean square (rms) velocities into interval velocities in the depth domain. Then, we merge the near-surface velocity-depth model with the initial model as the starting velocity model for anisotropic reflection tomography. We tested the proposed method on a complex 2D synthetic data example, and we then applied it to a 3D field data set from foothills of western China.

Principle of integrated tomography

Zhu et al. (2001, 2003) and Song et al. (2014), among others, propose joint tomography combining refraction or turning-ray tomography and reflection tomography to build an entire velocity model for depth migration. Turning-ray tomography has been conventionally used to calculate statics, which is also referred to as tomostatics (Zhu et al., 1992; Bell et al., 1994; Stefani, 1995; Zhang et al., 2006). In turning-ray tomography, the medium to be imaged is generalized into a continuous medium such that the first arrivals recorded at the surface need not be associated with refractors that have strong velocity contrasts. Turning-ray tomography inverts for a velocity model by minimizing misfits between observed first-break times and calculated travel times from turning rays. Because a continuous medium is assumed, the inversion results in a grid-based model. Usually, turning-ray tomography can robustly invert models with a depth up to one-fourth of the recording aperture (signed offsets). Very often, the turning ray penetrates deeper than the refraction ray because refraction requires velocities to increase with depth, whereas the turning wave does not need this requirement, provided that the earth has an overall positive velocity gradient due to compaction of rocks and the recording aperture is sufficient enough to allow rays turning back to the surface. We can use this model as a good estimation of the near-surface model combined with reflection tomography. However, in practice, we need to select maximum depths of reliable velocities according to the ray density for every location.

[1]Tarim Oilfield Company, PetroChina, Korla, China. E-mail: tianjun-tlm@petrochina.com.cn; penggx-tlm@petrochina.com.cn.
[2]Forland Geophysical Services (FGS), Houston, Texas, USA. E-mail: jjiao@forlandgeo.com; yyan@forlandgeo.com; xzhu@forlandgeo.com.

Manuscript received by the Editor 14 January 2018; revised manuscript received 11 August 2018; published ahead of production 07 September 2018; published online 9 November 2018. This paper appears in *Interpretation*, Vol. 6, No. 4 (November 2018); p. SM63–SM70, 19 FIGS.
http://dx.doi.org/10.1190/INT-2018-0005.1.

Reflection tomography in the postmigration domain uses depth residuals among traces within a common-image gather (CIG) generated from prestack depth migration (Stork, 1992; Jiao et al., 2009, 2010; Sherwood et al., 2011). The residuals are distributed along reflection rays. By minimizing the residuals, reflection tomography inverts for the perturbation of velocity and other anisotropic parameters and then updates models according to the previous models. Reflection tomography is an iterative process of prestack depth migration and tomographic inversion until the residuals are diminished because linearization is applied.

Because the near-surface velocity-depth model derived from turning-ray tomography is more accurate and has higher resolution than that from reflection tomography beneath the surface, we keep this model unchanged during the early stages of iterations in the integrated tomography. To account for the errors associated with the picked first arrivals for turning-ray tomography and combine both models seamlessly, we allow reflection tomography to update shallow and deep velocities simultaneously in the later stage of iterations. Reflection tomography is a global inversion. At early stages of model building, errors in estimation of models are larger in deeper areas than in shallower areas. The errors in deeper areas affect shallower areas. To avoid error transfer to the near-surface model derived by the turning-ray tomography, the near-surface model is masked in the first several iterations. After a few iterations of reflection tomography, the errors are reduced. Then, reflection tomography updates the velocity and anisotropic parameters in the shallower and deeper areas.

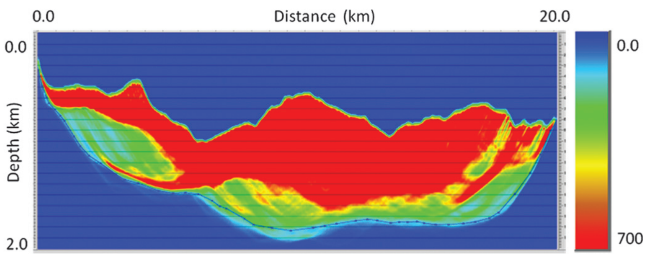

Figure 1. Ray density from turning-ray tomography. The dotted line in the deeper part is the horizon for the maximum depth of the reliable velocities.

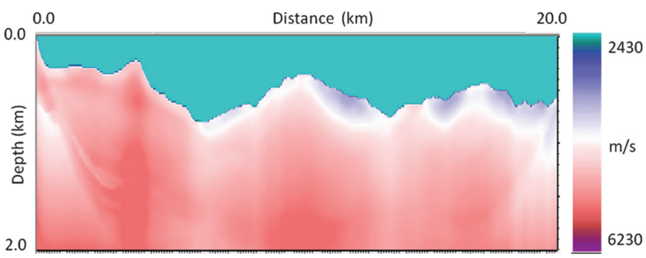

Figure 2. Inverted near-surface model from turning-ray tomography.

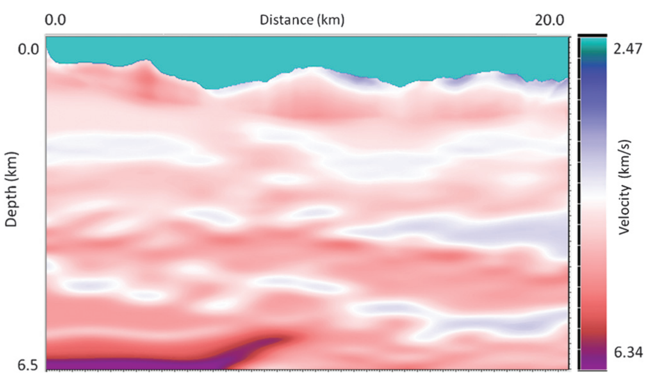

Figure 3. The combined initial model for reflection tomography. The shallow part is from the inverted near-surface model from turning-ray tomography, and the deep part is from the true velocity model with heavily smoothing and scaling.

Synthetic data example

We first applied the proposed method and workflow to a 2D synthetic data set, which simulates the Canadian Foothills (Boonyasiriwat et al., 2009). The model has a dimension of 20 km in the crossline direction and 6.5 km in depth. It has a rugose topography with an elevation relief up to 700 m, and the subsurface geologic structures are also complicated. The very specific feature of the model is that there are no reflection layers within 600 m underneath the surface, which makes it very difficult to derive the near-surface model by reflection tomography. We first picked the first arrivals from common-shot gathers, and then we performed turning-ray tomography. Figures 1 and 2 show the ray density and inverted near-surface velocity-depth model, respectively. According to the distribution of the ray density in Figure 1, we picked a horizon as the maximum depth for reliable velocities. The maximum thickness of the inverted model is approximately 1200 m from the topography. To create an initial model for prestack depth migration, we heavily smoothed the true velocity model in the horizontal and vertical directions, scaled the velocities by 0.95, and then combined that with the near-surface model. At the suture zone (defined by the dotted line based on the ray-density quality control [QC] plot as shown in Figure 1), tapering was applied to avoid abrupt changes. This combined model is presented in Figure 3.

Beginning with the initial combined model, we perform migration and reflection tomography iterations. We use Kirchhoff prestack depth migration to generate CIGs in the offset-depth domain. The offsets of gathers are from 100 to 7900 m with an increment of 200 m, and the depth is 6500 m with an interval of 5 m. Figure 4 shows the CIGs at selected crosslines after prestack depth migration using the initial velocity model. Most events are curved up and also show nonhyperbolic residual moveout because the true velocities are scaled by 0.95 and the model has strongly vertical and lateral velocity variations. The stacked migration from the initial model is shown in Figure 5.

In this example during the first three tomographic iterations, we keep the near-surface part unchanged by applying masking function in the inversion. Later, we allow reflection tomography to update near-surface and subsurface areas simultaneously. We find that reflection tomography adds more details into the near-surface model. After several iterations, the flatness of the CIG has been improved significantly, and more details are revealed for the velocity model. Figures 6 and 7 show the selected CIGs and stack from the final inverted model in Figure 8. For comparison, we also present the true velocity model and the corresponding stacked migration section in Figures 9 and 10, respectively. Although the inverted model is quite smooth, it shows the major features of the true model. Comparing stacked migrations from the initial model, the inverted model, and the true model, the image from the inverted model removes the "fake structures" marked by the white and yellow rectangles and caused by inaccurate initial model. The overthrust feature in the middle of the model (the circle in Figure 8) after the integrated tomography is also evident.

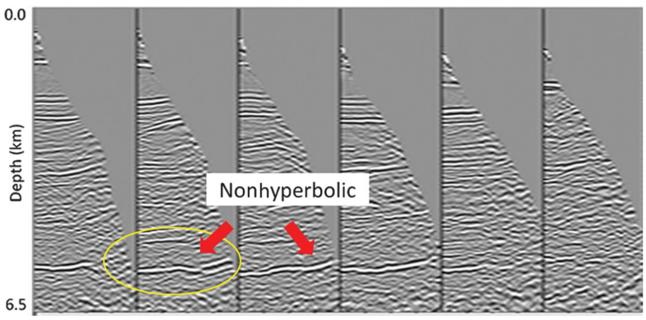

Figure 4. The selected CIGs using the integrated initial velocity model. The arrows show the nonhyperbolic residual moveout. The gathers are in the depth-offset domain. The offset is from 100 to 7900 m with a 200 m increment.

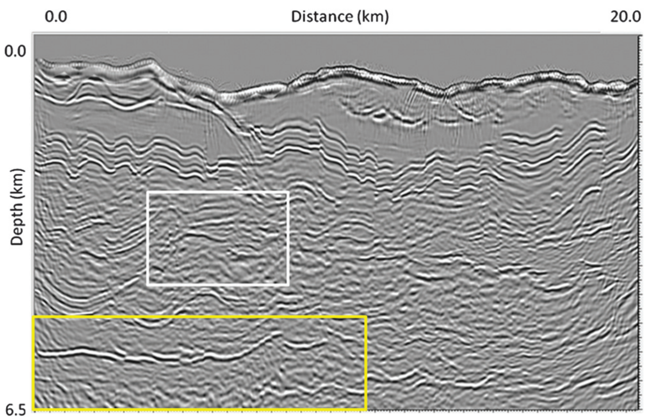

Figure 5. Stacked migration from the initial velocity model. The rectangle marks show the distortion of the subsurface image because of errors in the velocity model.

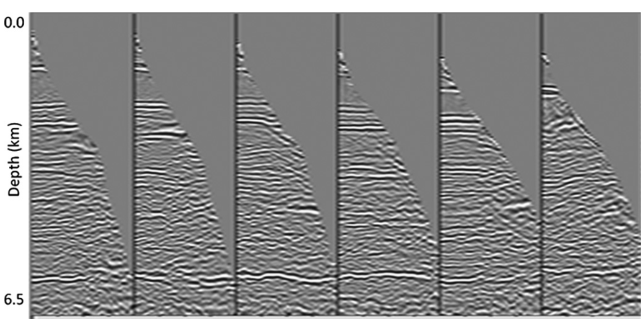

Figure 6. The selected CIGs using the updated velocity model from the proposed integrated tomography after several iterations. The gathers are in the depth-offset domain. The offset is from 100 to 7900 m with a 200 m increment.

Field example

We have applied the proposed methods to several field projects. Here, we take Keshen project as an example. The area is located at the Tarim Basin, northwestern China, where a set of thrust faults were pushed southward by the northern Tianshan orogeny, which resulted in rugged topography with steep slopes, dipping

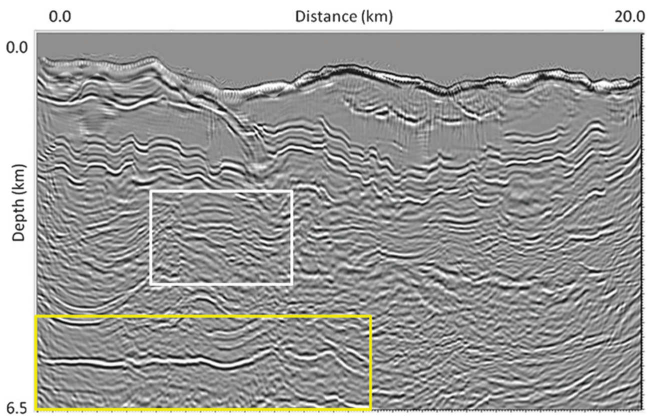

Figure 7. The stacked migration using the updated velocity model from the proposed integrated tomography after several iterations. The rectangle marks show the distortion of the subsurface image because of errors in the velocity model.

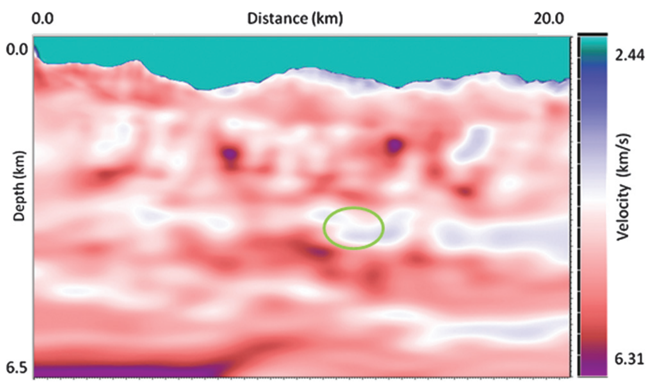

Figure 8. The updated velocity model from the proposed integrated tomography after several iterations. The circle shows the inverted overthrust feature corresponding to the true model.

outcrops (maximum more than 80°), and the relative elevation variation from 500 to 1000 m. Figure 11 shows a schematic geologic vertical section for the studying area. Figure 12 shows the elevation map of the study area. The near-surface morphology of the study area is known to have isolated high-velocity conglomerate

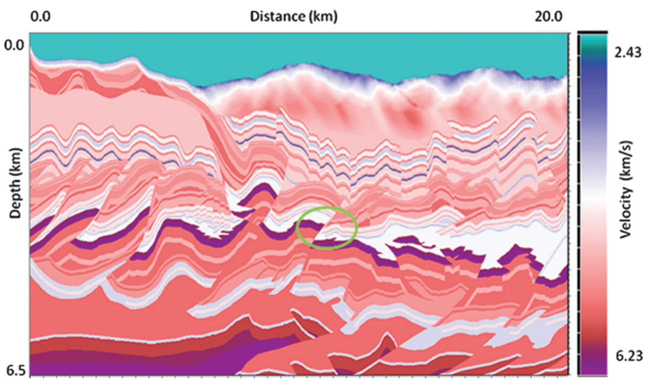

Figure 9. The true velocity model derived from the Canadian Foothills. This model is used to generate synthetic seismic shots for this study. The circle shows the overthrust.

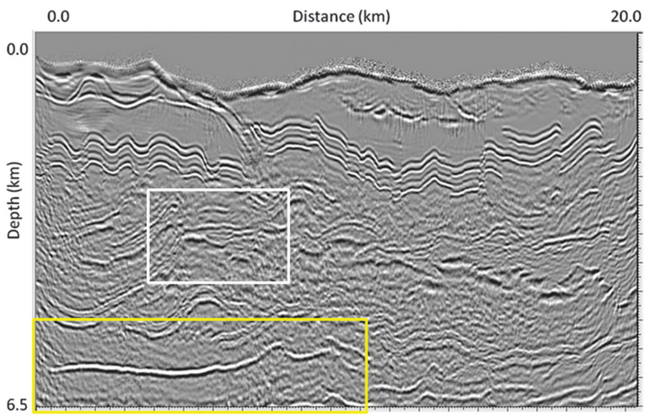

Figure 10. The stacked migration using the true velocity model. The rectangle marks corresponding to ones in the other stacked sections.

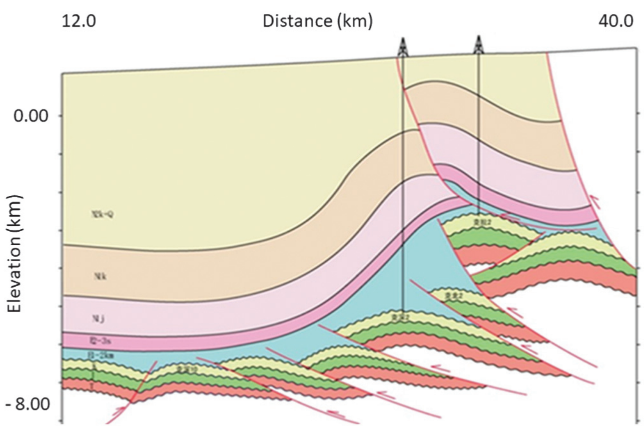

Figure 11. A schematic geologic section for the studying area.

rocks in the foreland basin surrounded by weathered sediments. The targeted zones are at depths of approximately 7 km underneath the conglomerate rocks.

To estimate more accurate models and obtain images with high fidelity, we first derive the near-surface velocity-depth model and combine it with the legacy depth model. Then using the combined model as the starting model, we perform iterative reflection tilted transverse isotropy (TTI) tomography and prestack depth migration for anisotropic model building. The resultant near-surface model is shown in Figure 13a for one inline and in Figure 13b for the depth slice at a depth of 900 m. The marked high-velocity zone corresponds to conglomerate rocks, and it is consistent and compatible with the geologic background of the study area. A "reliable depth" from the turning-ray tomographic solution can reach approximately down to 1500 m from the topography (the dashed line in Figure 13a), which is much deeper than the one from conventional refraction inversion. Figure 14 shows the combined model. From the final datum to the surface, a constant replacement velocity is used. From the surface to the reliable depth (the red dashed line in Figure 14), we use the velocity from the turning-ray tomography. The deeper area is filled with the legacy model previously obtained. There is a transient zone between the near-surface and legacy models.

During first three iterations, we keep the near-surface model unchanged, whereas we update both models in the last two iterations. Figure 15 compares the final velocity model with the starting one located at one inline. Figure 16 compares the initial epsilon and inverted epsilon overlaid with the stacked prestack depth migration (PSDM), respectively, located at the same inline as shown in Figure 15. The updated models reveal more details. After TTI tomography, the near-surface velocities are reduced, whereas the anisotropic parameter epsilon is increased. Although the initial epsilon is

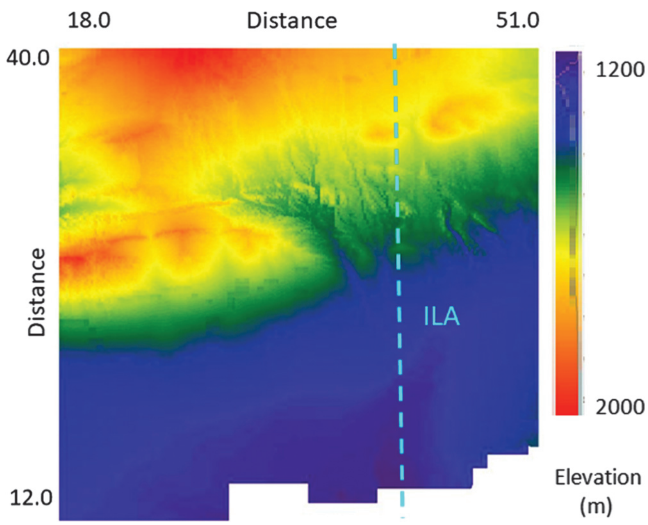

Figure 12. Elevation map of studying area. The white dashed line presents the inline ILA.

constant, the inverted epsilons vary vertically and laterally consistent with imaged structures. The inverted epsilons are larger in dipping layers than that in horizontal layers. At shallow areas, inverted epsilons are larger than the initial ones. This case demonstrates that isotropic turning-ray tomography leads to higher estimation of velocity due to the existence of anisotropy. The migrated results from the updated models are shown in Figure 17. This representative inline is overlaid with Well KS12. The new apex of the structure (the blue line cutting through) is now on the right side of the previously drilled location (the yellow dashed line), several hundred meters apart. The well drilled previously missed the target, and only water was discovered in the reservoir. A new well location was suggested according to the current processing.

After the application of TTI reflection tomography (Zhou et al., 2011), the velocities near the surface have been slightly reduced. This is because in isotropic turning-ray tomography, which was used in this study, the near-surface velocities will be overestimated if the

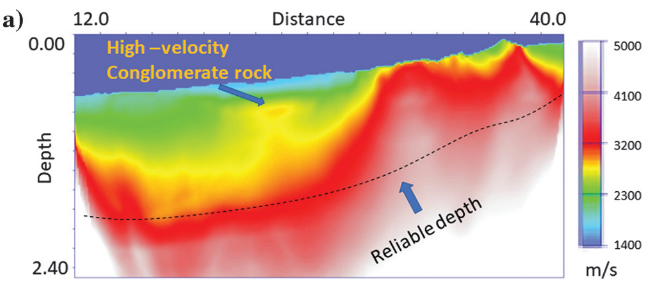

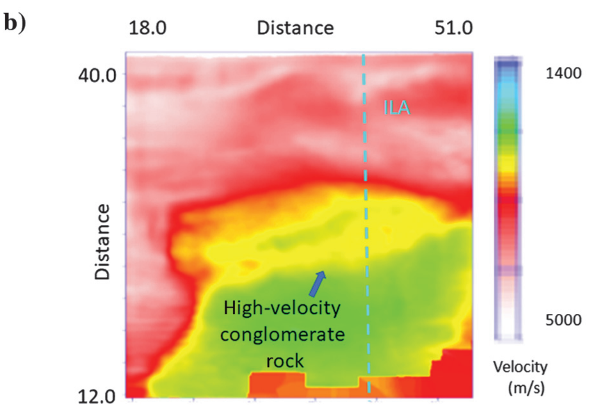

Figure 13. (a) Near-surface model derived from turning-ray tomography at inline ILA. (b) Depth slice at 900 m of near-surface model derived from turning-ray tomography.

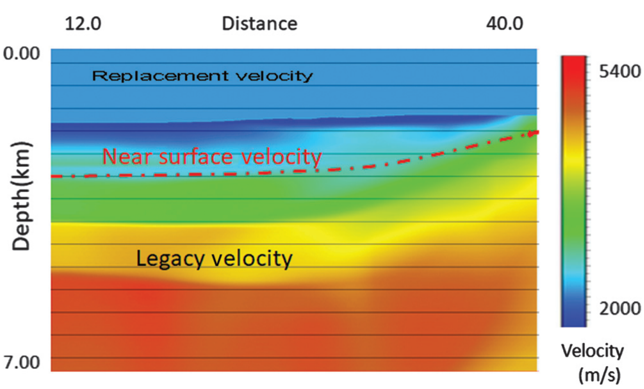

Figure 14. Initial model combining near-surface model derived from turning-ray tomography and legacy model.

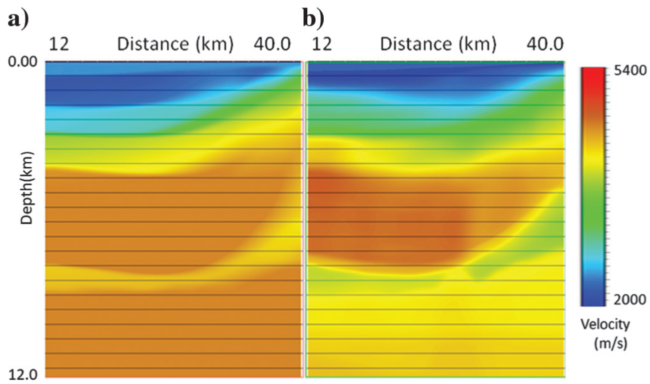

Figure 15. Velocity (a) before and (b) after integrated tomography update.

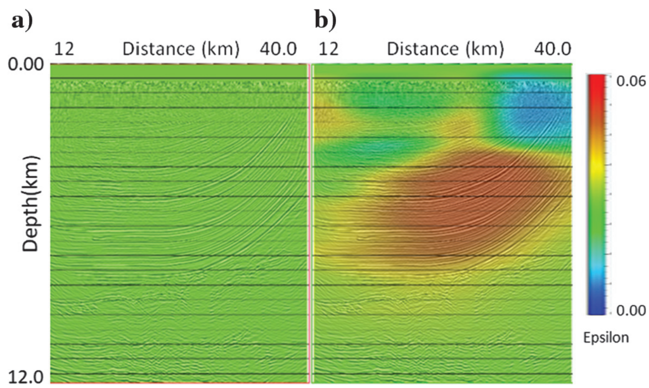

Figure 16. Stacked PSDM overlaid with the (a) initial and (b) inverted anisotropic epsilons, respectively.

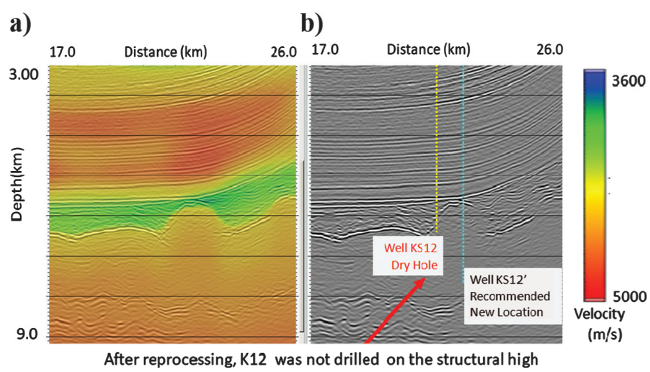

Figure 17. Location of Well KS12 on a representative TTI PSDM section. The new apex of the structure (the blue line cutting through) is several hundred meters away from the previously drilled location (the yellow dashed line), suggesting a new well location. (a) The updated velocity overlaid by the image and (b) theimage only.

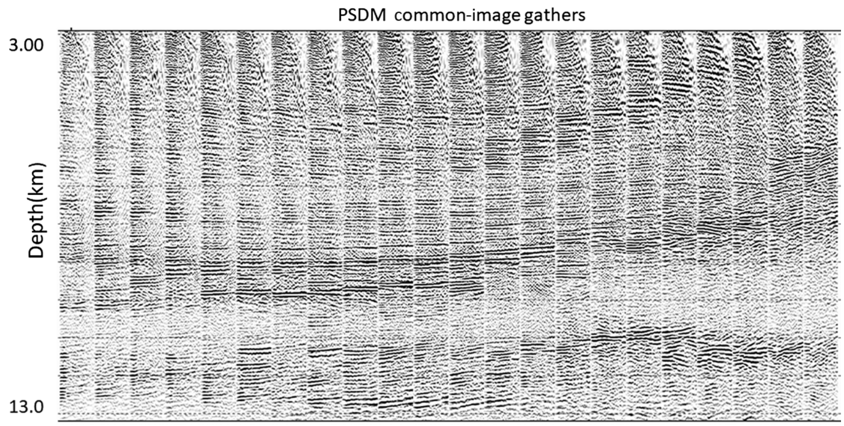

Figure 18. The CIGs located at several crosslines at inline ILA generated by PSDM using the initial models. The gathers are in the offset and depth domains. Some events curve down, and others curve up.

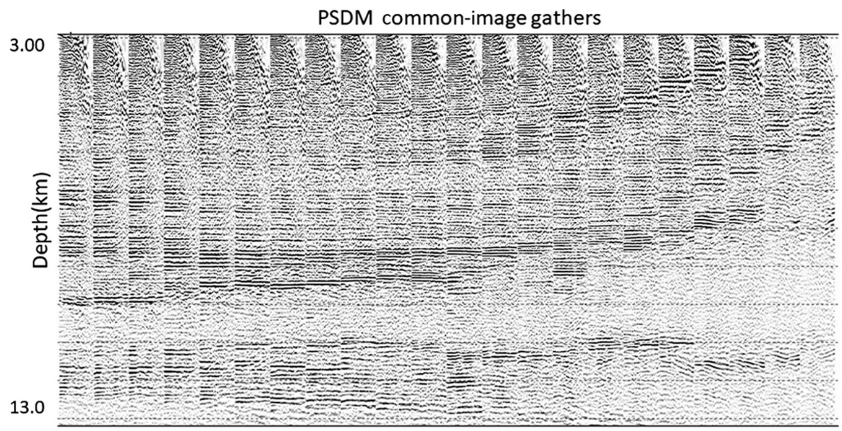

Figure 19. The CIGs located at several crosslines at inline ILA generated by PSDM using the updated anisotropic models. The gathers are in the offset and depth domain. The flatness of the events improves significantly overall.

media near the surface are anisotropic. Turning rays contain a substantial horizontal component. TTI reflection tomography can compensate for the horizontal component. Figures 18 and 19 compare the CIGs from the initial models and the updated models. The flatness of the events improves significantly overall, which demonstrates that anisotropic tomography is necessary to derive multiple anisotropic parameters for imaging.

Conclusion

We have proposed a method of integrated turning-ray and reflection tomography to build models, using a different constraint strategy. The proposed method faces the difficulty of estimating the near-surface model in land seismic imaging. We first use turning-ray tomography to derive the near-surface velocity-depth model using the first arrivals as input. Then, reflection tomography is performed to invert for the subsurface model with the near-surface model masked at first several iterations. During later iterations, the near and subsurface models are updated. We found that near-surface velocities are decreased after integrated inversion. The percentage of velocity reduction depends upon the degree of anisotropy near the surface. We have applied the proposed method to the complex 2D synthetic data set and 3D field data set successfully. Both examples show that turning-ray tomography produces more accurate and higher resolution near-surface velocity-depth models with deeper penetration than that from conventional refraction inversion, and the integrated turning ray and reflection tomographic inversion lead to the geologic plausible models thence producing a subsurface image with higher fidelity.

Acknowledgments

We thank A. Bertagne, S. Yang, L. Fu, B. Yang, and J. Gillooly for valuable discussions. We also thank the Tarim Oilfield Company of PetroChina and Forland Geophysical Services for permission to publish this work. Constructive suggestions and comments from the anonymous reviewers are very much appreciated.

Data and materials availability

Data associated with this research are available and can be obtained by contacting the corresponding author.

References

Bell, M. L., R. Lara, and W. C. Gray, 1994, Application of turning-ray tomography to the offshore Mississippi Delta: 64th Annual International Meeting, SEG, Expanded Abstracts, 1509–1512, doi: 10.1190/1.1822824.

Boonyasiriwat, C., P. Valasek, P. Routh, and X. Zhu, 2009, Application of multiscale waveform tomography for high-resolution velocity estimation in complex geologic environments: Canadian Foothills synthetic data example: The Leading Edge, **28**, 454–456, doi: 10.1190/1.3112764.

Jiao, J., S. Lin, C. Zhou, S. Brandsberg-Dahl, K. Schleicher, and H. Tieman, 2009, Multi-parameter controlled automatically picking and variable smoothing for tomography with fast 3D beam prestack depth migration: 79th Annual International Meeting, SEG, Expanded Abstracts, 3989–3993, doi: 10.1190/1.3255702.

Jiao, J., C. Zhou, S. Lin, D. Van der Burg, and S. Brandsberg-Dahl, 2010, Velocity model building strategy for multi-azimuth surveys: 80th Annual International Meeting, SEG, Expanded Abstracts, 4380–4384, doi: 10.1190/1.3513789.

Sherwood, J., J. Jiao, H. Tieman, K. Sherwood, C. Zhou, S. Lin, and S. Brandsberg-Dahl, 2011, Hybrid tomography based on beam migration: 81st Annual International Meeting, SEG, Expanded Abstracts, 3979–3983, doi: 10.1190/1.3628037.

Song, M., X. Liu, X. Han, D. Wang, S. Yang, and C. Hinz, 2014, Combining diving-wave tomography and prestack reflection tomography for complex depth imaging — A case study from mountainous western China: The Leading Edge, **33**, 868–874, doi: 10.1190/tle33080868.1.

Stefani, J. P., 1995, Turning-ray tomography: Geophysics, **60**, 1917–1929, doi: 10.1190/1.1443923.

Stork, C., 1992, Reflection tomography in the post migrated domain: Geophysics, **57**, 680–692, doi: 10.1190/1.1443282.

Zhang, J., O. Yilmaz, and N. Dai, 2006, First-arrival tomostatics and residual statics for near-surface corrections: Proceedings of the CSPG-CSEG-CWLS Convention, 317–321.

Zhou, C., J. Jiao, S. Lin, J. Sherwood, and S. Brandsberg-Dahl, 2011, Multiparameter joint tomography for TTI model building: Geophysics, **76**, no. 5, 183–190, doi: 10.1190/geo2010-0395.1.

Zhu, X., A. Huffman, and J. Castagna, 2003, Tomography for enhanced geopressure prediction and depth imaging: Proceedings of the SPG/SEG Conference.

Zhu, X., D. P. Sixta, and B. G. Angstman, 1992, Tomostatics: Turning-ray tomography + static corrections: The Leading Edge, **12**, 15–23.

Zhu, X., K. D. Wyatt, and A. Lau, 2001, Turning-ray tomography and tomostatics: 71st Annual International Meeting, SEG, Expanded Abstracts, doi: 10.1190/1.1821921.

Tian Jun received a Ph.D. (2005) in mineral census and exploration from Southwest Petroleum Institute. He has more than 30 years of petroleum exploration experience. After graduating from East China Petroleum Institute, he worked for Xinjiang Petroleum Administration Bureau as a geophysical interpreter. In 1989, he started to work for Tarim Oilfield Company and focused on geophysical technologies and geological comprehensive research. He is now the vice president of PetroChina Tarim Oilfield Company, responsible for petroleum exploration and information technology. He organized the geophysical technical research in both foreland and platform-basin areas in Tarim Basin. He organized mountain seismic research in Kuqa foreland basin, initiated the structural modeling method based on fault-related fold theory, and improved and developed the geological theory of petroleum exploration in Kuqa foreland basin. He also organized the technical task force on seismic reservoir description in fracture-vug carbonate rocks and started the integrated exploration and development approach for complex reservoirs. He is the major contributor in the discovery of the 1×10^{12} m^3 reserves gas fields in the Kuqa area and the discovery of Halahatang and Tazhong giant oil and gas fields with reserves of more than 1 billion tons. His research achievements won three second prizes of the National Science and Technology Progress Award and 15 provincial and ministerial-level awards. He also received the distinguished achievement award from CNPC in 2005, and the fifth Huang Jiqing Young Geology Award in 2010.

Peng Gengxin is a professor-level senior engineer and chief engineer of the Research Institute of Exploration and Development at PetroChina Tarim Oilfield Company. He has been engaged in seismic data processing and interpretation research and technology control in Tarim for 27 years and has participated in and undertaken many major research projects from the Chinese government and PetroChina. He has won 10 awards at or above the provincial level, seven national technical invention patents, three coauthored monographs, and has published more than 30 papers.

Junru Jiao received a B.S. (1982) and an M.S. (1989) in geophysics from the China University of Petroleum and a Ph.D. (2001) in geologic sciences from the University of Texas at Austin, Texas. He is a recognized expert in tomography, depth imaging, and data processing. Early in his career from 1982 to 1997, he worked for the Bureau of Geophysical Prospecting (BGP) where he gained experience in all aspects of exploration that included seismic acquisition design, field QC, seismic data processing from tape loading to final migration, and research into software development for geophysical algorithms in signal enhancement and imaging. From 1996 to 1998, he held the position of chief geophysicist for the Department of Research, GRI, BGP and from 2001 to 2011, manager of the velocity section for PGS. From 2011 to 2016, he was employed by Repsol as advisor research geophysicist. Currently, he serves as vice president of imaging for Forland Geophysical Services in Houston. His most significant contribution to geophysics is his ability to identify and create new approaches to geophysics algorithms, implement those approaches into software, and ultimately apply those approaches into production. Several of his most notable achievements resulted in patents for anisotropic model building and demigration. He also had more than 20 papers published over the past 20 years.

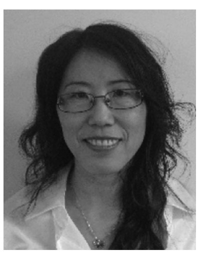

Grace Yan received a B.S. (1990) in geophysics from China University of Petroleum and an M.S. (2001) in geophysics from the University of Calgary. She has more than 25 years of experience in oil exploration, oil companies, and service companies. She worked at Xinjiang Petroleum Exploration Company for eight years, GXT

Canada for five years, CGGVeritas as senior geophysicist and team leader for six years, and ConocoPhillips as staff processing geophysicist for four years. Her specialties are prestack time and depth migration, tomographic velocity update integrating wells, horizon picking, and VVAZ/AVAZ processing. Currently, she is working at Forland Geophysical Services as the vice president of processing.

Xianhuai Zhu received a B.S. in geophysics from China University of Petroleum and a Ph.D. (1990) in geosciences from the University of Texas at Dallas. He has more than 30 years of experience in the oil and service company industry. He had been with Anadarko (formerly UPR), PGS, Fusion Petroleum Technology, and ConocoPhillips. He started his career from a field of seismic crew and worked for SINOPEC Geophysical Research Institute (SGRI) in China before moving to the United States. From 1985 to 1986, he was a visiting scientist at Cornell University in Ithaca, USA. In 2016, he founded Forland Geophysical Services Company (FGS) in Houston, which deals with developing and applying advanced technologies for land, shallow-water, and OBN seismic data acquisition, imaging, and interpretation. From SEG, he received the Reginald Fessenden Award in 2012 for his pioneering work on turning-ray tomography and tomostatics, and the Life Membership Award in 2018. In 1999, he received the Best Paper Award on “Recent advances of multicomponent processing.” He was the director-at-large for the SEG board of directors during the period of 2014–2017 and the first vice president of the Geophysical Society of Houston (GSH) during 2017–2018.